Chapter 6

Lead Zirconium Titanate Films and Devices Made by a Low-Temperature Solution-Based Process

Phan Trong Tue and Yuzuru Takamura

Additional information is available at the end of the chapter

http://dx.doi.org/10.5772/intechopen.79378

Abstract

As the most important multifunctional oxide material, lead zirconium titanate (PZT) has a diverse range of applications such as piezo actuators, ferroelectric nonvolatile memories, sensors, and transducers due to its excellent structural and electrical properties. However, it generally requires a high annealing temperature (above 600°C) to attain the desired properties, which hinders the integration of PZT with silicon-based Complementary Metal Oxide Semiconductor (CMOS). Therefore, the fabrication of PZT films by a chemical solution deposition (CSD) at temperatures compatible with Si-CMOS technology or even with polymeric substrate for flexible electronics would be of high technological interest. So far, different strategies to decrease the crystallization temperature of CSD-derived PZT films have been studied. This chapter presents a critical review on the low-temperature solution-processed PZT films and devices, and addresses challenges for fundamental understanding and practical integration of multifunctional PZT in devices. In the first part, recent advances in fabrication of CSD-derived PZT films at a low temperature are thoroughly reviewed. The second part discusses various techniques for patterning PZT into micro-nano-sized patterns. Lastly, some potential applications of the low-temperature CSD-derived PZT films and devices are demonstrated.

Keywords: lead zirconium titanate (PZT), ferroelectric, ferroelectric nonvolatile memory, piezoelectric actuator, solution process, low-temperature deposition

1. Introduction

Highly integrated nano-ferroelectric/piezoelectric devices with Si-CMOS technology require a low-processing temperature (≤450°C) of ferroelectric/piezoelectric films [1]. Among ferroelectric/piezoelectric materials, lead zirconium titanate (PZT) [2] appears as the most promising candidate because of its excellent structural and electrical properties, in addition to its

IntechOpen

© 2018 The Author(s). Licensee IntechOpen. This chapter is distributed under the terms of the Creative Commons Attribution License (http://creativecommons.org/licenses/by/3.0), which permits unrestricted use, distribution, and reproduction in any medium, provided the original work is properly cited. CC BY

relatively low processing temperature (~600°C) compared to organic, lead-free, and the other inorganic materials [3, 4].

Many efforts have been done for lowering the process temperature of device-quality PZT films to below 450°C such as the chemical vapor deposition [5], pulse laser deposition [6], and sputtering [7]. However, most of these technologies are costly and complicated, which are not suitable for practical applications. On the other hand, the chemical solution deposition (CSD) technique offers many advantages such as simplicity, low-cost, large area deposition, and feasibility of material compositional control. Many low-temperature CSD methods, including tailoring precursor solution [8, 9], seeding the film [10], hydrothermal annealing [11], and better lattice matching [12], have been investigated, but all provide insufficient film quality and compromised properties. Hitherto, the relatively successful approaches have been microwave annealing [13], localized heating by pulse laser [14], and ultraviolet-assisted annealing [15]. Nevertheless, microwave heating results in damage of CMOS circuits, while the costly pulse laser processing is unfavorable for industrial application.

This chapter presents a critical review on the low-temperature solution-processed PZT films and devices since last 15 years, and addresses challenges for fundamental understanding and practical integration of multifunctional PZT films in devices. Database collection was performed using major searching engines such as ISI Web of Science (Thomson Reuters) and Google Scholar. In the first part, recent advances in fabrication of CSD-derived PZT films at a low temperature (≤450°C) using chemical and physical approaches are thoroughly reviewed. The second part discusses various techniques such as wet/dry-etching, lift-off, and imprinting for patterning PZT into micro-nano-sized patterns. Lastly, some potential applications of the low-temperature CSD-derived PZT films and devices for sensor/actuator and energy harvesting are demonstrated.

2. Recent progress of low-temperature PZT films fabricated by a chemical solution deposition (CSD) method

2.1. Chemical pathway

2.1.1. Seeded diphasic sol-gel (SDSG) precursors

It is evident from literatures that there have been few studies of the phase evolution of PZT films at temperature normally considered suitable for pyrolysis (350–450°C) rather than crystallization (600°C). The reaction pathway from nucleation to full growth of perovskite PZT phase plays an important role in optimizing and lowering process-temperature of sol-gel derived films.

To understand the mechanism of transformation from the nucleation to the growth of perovskite PZT, microstructural development, crystallinity and electrical properties of low-temperature pyrolyzed PZT films (<400°C) were systematically investigated. The films were prepared on Pt-coated Si substrates by a sol-gel route, in which different concentrations of nanometric PZT powders were dispersed in the sol (seeded precursor) [10, 16, 17]. It was found that the formation of perovskite phase was facilitated by the seeds as a result of the reduced activation

http://dx.doi.org/10.5772/intechopen.79378

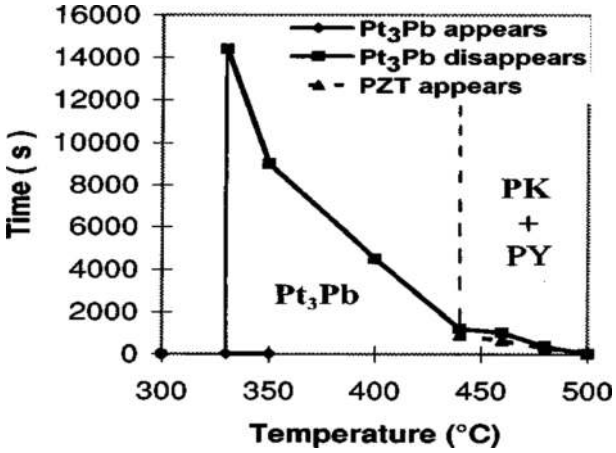

Figure 1. Temperature-time-texture diagram for the metastable $PbPt_3$ phase and perovskite PZT for the three-layer films dried at 200°C [19].

energy [17]. The seeded PZT films showed a lesser (111)-preferential orientation, greater nucleation density, and a better ferroelectricity. The formation of the metastable intermetallic Pt_xPb interlayer, between the film and the Pt electrode layer, was also observed. However, the local random perovskite nucleation might result in the decreased (111) orientation of the seeded films [18]. The obtained dielectric permittivity (ε), remnant polarization (P_r), and coercive field (E_c) of the 430°C-pyrolyzed seed-PZT film were 500, 6.71 μC/cm^2, and 80 kV/cm, respectively.

2.1.2. Formation of an early stage seeded PbPtx layer

It has been reported that an intermetallic $PbPt_3$ phase is formed in the early stages of pyrolysis for PZT thin films deposited on a platinized substrate, which greatly influences on crystallization temperature, microstructure, and electrical properties of resulting films [18, 19]. This metastable phase forms at around 330°C and disappears as elevated heating (**Figure 1**). The pyrolysis and annealing conditions as well as the film thickness determine the formation of this intermetallic phase. These conditions impact on the reduction of Pb^{2+} into Pb, which drives the formation of the $PbPt_3$ phase. The perovskite nucleation was found on top of the intermetallic phase rather than directly on Pt. This explains why the formation of PZT(111) phase is facilitated by the intermediate ones (**Figure 2**) [20]. Due to very small lattice mismatch (0.4%) between the $PbPt_3$ and PZT phases, the nucleation activation energy might be reduced. As a result, well (111)-oriented perovskite PZT was able to be fabricated at 440–480°C. The PZT film exhibited a good quality with a pyroelectric coefficient of 1.8×10^{-4} Cm^{-2} K^{-1} and a P_r of 24 μC/cm^2 [20].

2.1.3. Solvothermal synthesis

Solvothermal synthesis is a method of crystallizing solution-derived materials under a high pressure and at a temperature higher than boiling temperatures of used solvents. The method

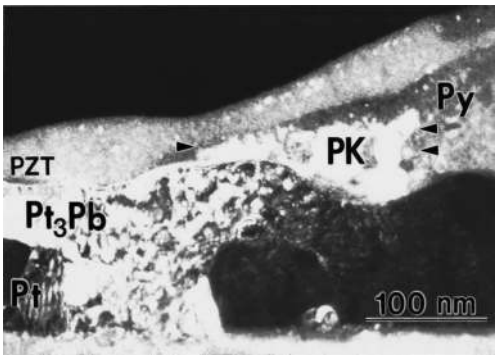

Figure 2. Dark-filed cross-section TEM for a film PZT/Pt/Ti/SiO_2/Si after annealing at 440°C [20].

has been widely used for the synthesis and growth of various materials and thin films such as metal oxides [21, 22].

The advantage of the solvothermal method is low reaction temperature, generally below 200°C. It is important to note that this temperature is lower than the Curie temperature of PZT (~200–350°C), and more than 400°C below the reaction temperature required by the other methods. When PZT is used as a transducer, the output force is proportional to the applied voltage, which increases as the film thickness increases. In this regard, the hydrothermal method is advantageous of making micrometer-thick film; consequently, it is a promising feature for developing a microactuator driver. In addition, since the material is synthesized in solution, the film is deposited on all surfaces of the substrate making it a three-dimensional (3D) structure. Such a 3D structure is advantageous not only for actuators but also for FeRAM applications.

The hydrothermal growth of polycrystalline PZT films on Ti-substrates in a two-step process (nucleation and growth) showed that alkaline medium such as KOH was important for the formation of the PZT solid solution [23, 24]. By slightly changing the reaction conditions, PZT films could be grown in a single step [25].

Hetero-epitaxial growth of PZT films on (001) $SrTiO_3$ (STO) was achieved at 90-150°C (**Figure 3(a)**) [26]. The growth proceeded with the formation of (100)-faceted islands and their coalescence. Full coverage was obtained upon hydrothermal treatment at 150°C for 24 h. However, both the (001) and (100) orientations were detected. In addition, ferroelectric properties were not able to be evaluated due to the lack of conductivity of the STO substrate and the peel-off morphology of the film [27]. Later, these issues were resolved by adjusting the position at which the substrate was suspended in the solution, and by the use a highly conductive $SrRuO_3$ film as a bottom electrode [28]. The $2P_r$ and E_c for PZT film on $SrRuO_3$/STO (001) were 17.1 μC/cm^2 and 36 kV/cm, respectively, and those of PZT on $SrRuO_3$/STO (111) were 32.7 μC/cm^2 and 59 kV/cm, respectively (**Figure 3(b)**).

2.1.4. Excluding pyrochlore phase formation

It is well known that PZT pyrochlore phase is formed at 300–400°C. Once this stable phase is developed, a high annealing temperature (>600°C) is required to transform it from the

http://dx.doi.org/10.5772/intechopen.79378

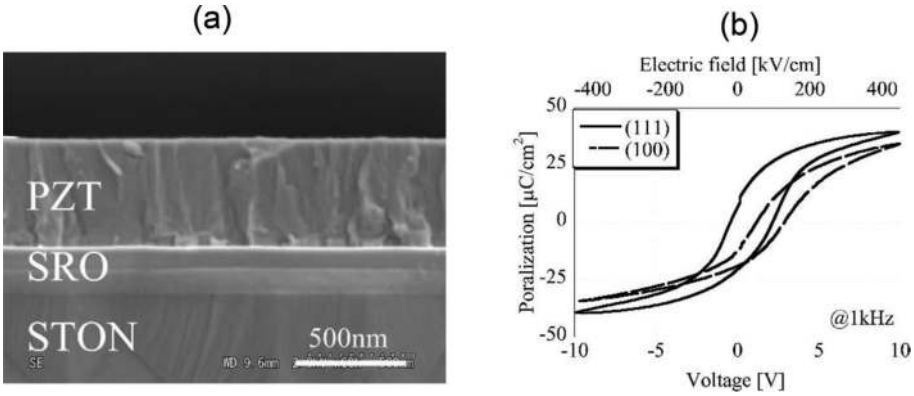

Figure 3. (a) Cross section of SEM image of the deposited PZT thin film on the $SrRuO_3$//STO (100) substrate. (b) Hysteresis curves for PZT thin films on $SrRuO_3$//STO (100) [26].

pyrochlore to a perovskite structure. A simple method for the crystallization of solution-processed PZT films at 400–450°C by intrinsic change in the crystallization path via circumventing the pyrochlore phase formation was reported [29]. The approach does not need any modification of the precursors nor special facilities. Conventionally, the spin-coated films are normally pyrolyzed at over 300°C for a complete removal of solvent and organic ingredients. However, by this pyrolysis step, the pyrochlore phase is subsequently formed. In this work, by lowering the pyrolysis temperature to a well-below pyrochlore temperature (i.e., 210°C), it was able to retain a proper amount of carbon atoms in the gel film as shown in **Figure 4(a)**. The remaining carbon acted as a reagent to reduce Pb^{2+} to Pb^0 when heated up to 400°C in subsequent annealing (**Figure 4(b)** and **(c)**). A significantly enhanced intensity of the $PbPt_x$ peak for the 210°C-pyrolyzed sample compared to the others indicated that larger amount of Pb^o was produced (**Figure 4(b)** and **(c)**). In the presence of sufficient organic carbon, Pb^{2+} was reduced to Pb^0, which spontaneously reacted with Pt to form the intermediate $PbPt_x$ phase at temperatures as low as 200°C. As a result, the lack of Pb^{2+} prevented the formation of this intermediate phase (**Figure 4(b)** and **(d)**) that accounts for the high-temperature crystallization of the perovskite phase in the conventional processes. The process was successfully demonstrated on several representative electrode materials (Au, stacked Pt/RuO_2, and RuO_2) in addition to Pt.

2.2. Physical pathway

2.2.1. Ultraviolet-assisted annealing

Recently, ultraviolet (UV)-assisted annealing has been applied for fabrication of various functional oxide thin films since the process is capable of facilitating organic decomposition and condensation of oxide network. Consequently, high-quality oxide thin films can be realized at a low temperature [30, 31].

Shimura et al. reported a low-temperature fabrication of PZT films using a thermal UV/O_3 annealing process [15]. A spin-coated PZT gel film was placed on a heated stage (200°C) and

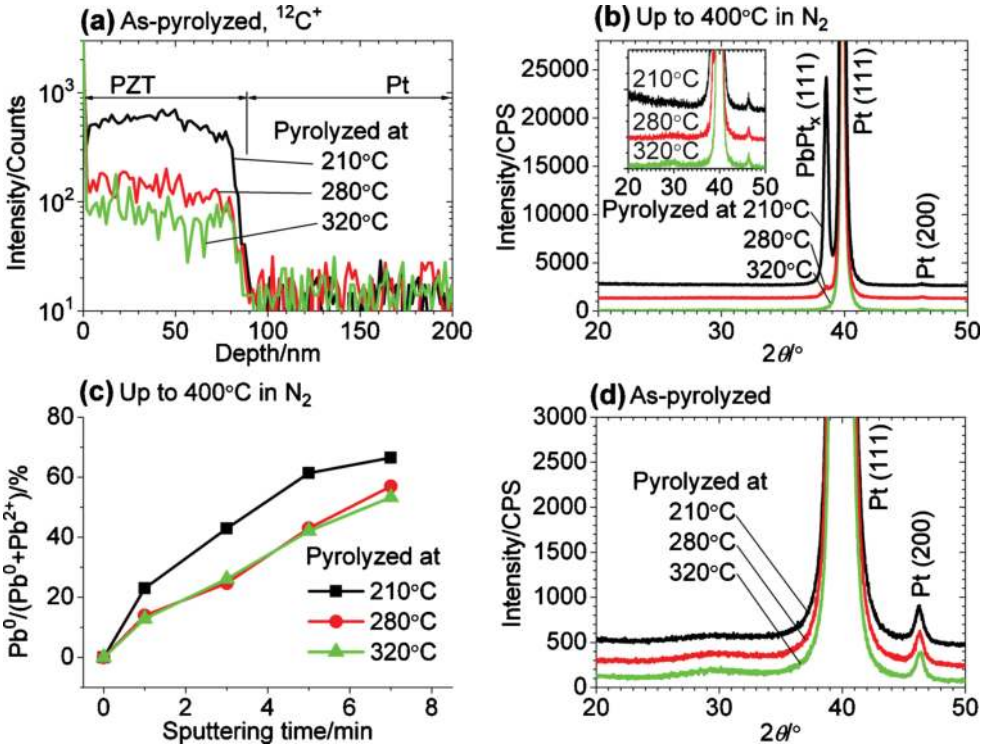

Figure 4. Effects of pyrolysis temperature on carbon content, valence state of Pb, and phase composition before perovskite crystallization. (a) SIMS analysis for carbon of the as-pyrolyzed samples. (b) XRD patterns for samples further heated to 400°C. (c) Percentages of reduced Pb. (d) XRD patterns for the as-pyrolyzed samples [29].

irradiated with UV light (185 and 254 nm) in O_3 ambient before crystallization (**Figure 5**). The thermal UV irradiation facilitated the decomposition of organic components. At a proper temperature, the organic residue such as carbon and hydrogen atoms created a reducing environment within the gel film, which prevented the pyrochlore structure development. As a result, the ferroelectric perovskite structure with (111)-preferential orientation was able to be achieved at 450°C (**Figure 6(a)**). The P_r, E_c, and leakage current of the PZT film were 23.6 μC/cm^2, 109.6 kV/cm (**Figure 6(b)**), and 10^{-6} A/cm^2, respectively [15]. Similarly, ferroelectric PZT films were fabricated on $LaNiO_3$ electrode at a low temperature of 450–480°C by a method assisted with UV irradiation [32]. The obtained film annealed at 480°C showed a P_r of 21 μC/cm^2 and leakage current of 9.71×10^{-8} A/cm^2 at 100 kV/cm, with good retention and high stability of photocurrent.

In order to enhance absorption in the UV-range, UV-absorber additives are normally added to precursor solutions such as "*photoactive sol*" (*Ph*) [33]. The dip-coated thin gel layer was irradiated under the UV-light, followed by rapid thermal annealing in O_2 atmosphere. Formation of highly reactive oxygen radical from ozonolysis facilitated the decomposition of organic components via breaking of the alkyl group-O bonds, resulting in a subsequent formation of the metal–O–metal bonds. As a result, ferroelectric perovskite structure can be obtained at 400°C. Furthermore, incorporation of nanoseeds into the *Ph* sol (*PhS*) increased

http://dx.doi.org/10.5772/intechopen.79378

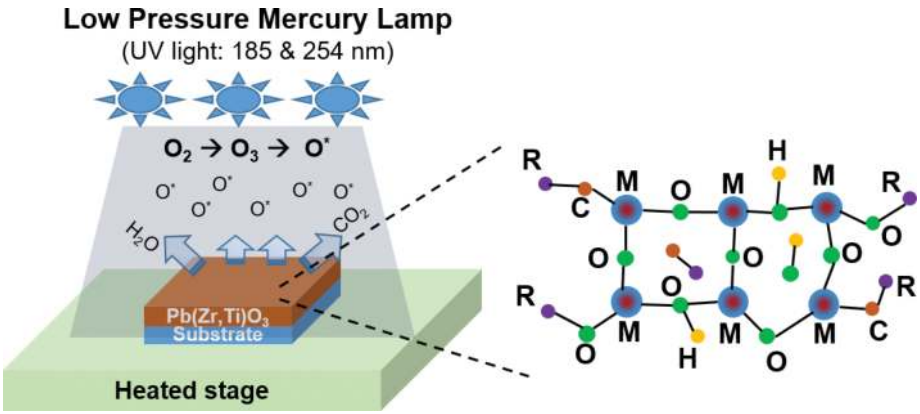

Figure 5. An illustration of UV treatment process for PZT films.

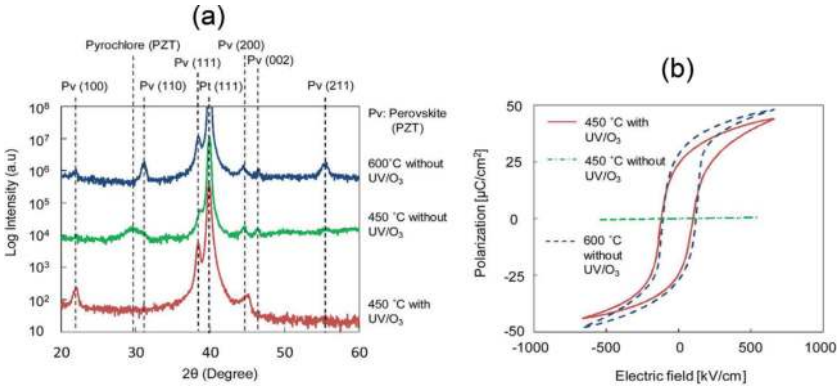

Figure 6. (a) XRD patterns and (b) hysteresis loop characteristics of PZT films prepared by conventional 600°C process and 450°C process with and without the UV/O_3 treatment [15].

the number of nucleation sites in the resulting film, which produced a further reduction of crystallization temperature [34]. The mechanism proposed for the low-temperature processing of *PhS*-PZT thin films is described in **Figure 7**. Combination of the enhanced UV-absorbance and internal nanocrystalline seeds led to a significant improvement in the formation of the PZT perovskite structure at a low temperature, which originated from a decrease of the Gibbs free energy barrier. The 350°C-PZT film deposited on a flexible PI substrate with a thickness of 190 nm, showed value of P_r ~ 15 μC/cm². This value is close to those reported for PZT films processed at temperature over 600°C, P_r ~ 20 μC/cm², and are higher than those reported for organic ferroelectric films, P_r ~ 10 μC/cm², both on rigid Si substrates.

2.2.2. Laser-assisted annealing

Laser annealing (LA) is an alternative technique for fast and low-temperature fabrication of PZT films. This technique uses focused high-energy laser beam in continuous or pulse mode

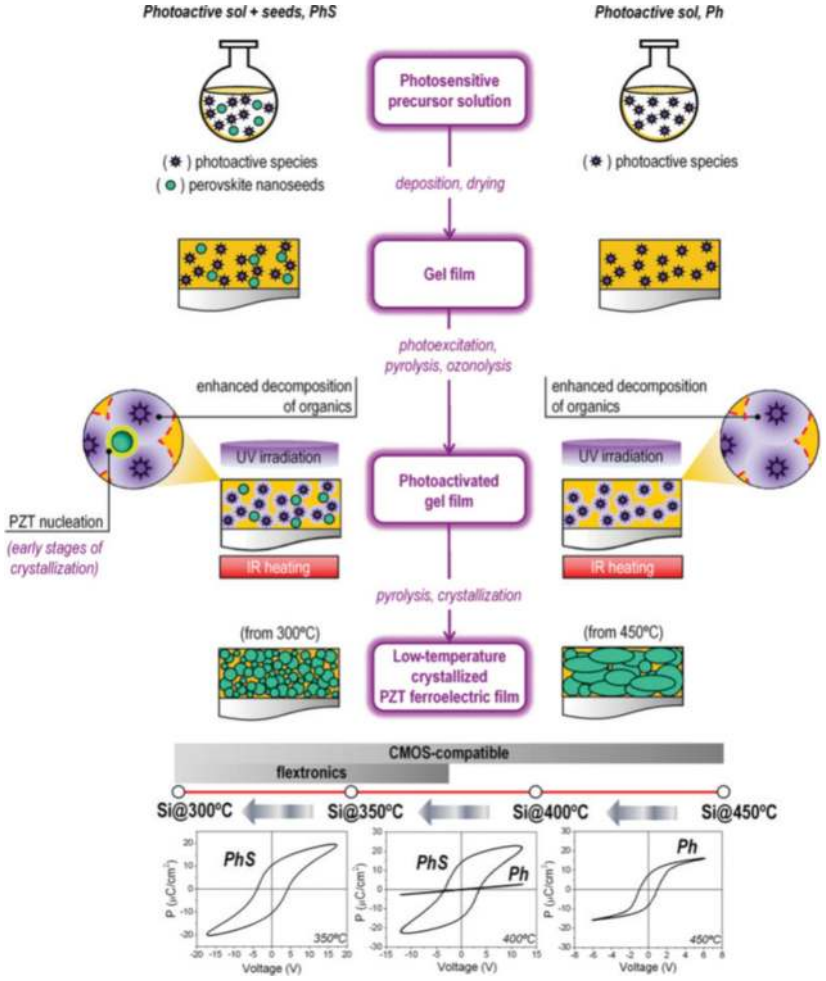

Figure 7. Mechanisms for the low-temperature processing of inorganic ferroelectric thin films using the activated *PhS* solutions [34].

to scan the desired film's areas to fuse and bond the powders into a layer of solid mass, and has been used in manufacture of solar cells and power devices. The advantages of LA include the flexibility in manufacturing composites with different geometries with assistance of computer, controllable sintering thickness depending on the laser energy and scanning speed, low influence on the substrate to create the possibility of processing PZT on low melting point substrates. However, LA technique is not suitable for a large area PZT sample due to the limitation of laser spot size (generally ~50 μm in diameter). Many researchers have attempted to apply this technique to PZT crystallization since three decades ago. Bharadwaja et al. [14] reported highly textured (001) and (111) $Pb(Zr_{0.52}Ti_{0.48})O_3$ thin films (300–350 nm thick) fabricated via excimer laser annealing (248 nm KrF pulsed excimer laser) on (111)$Pt/Ti/SiO_2/Si$

http://dx.doi.org/10.5772/intechopen.79378

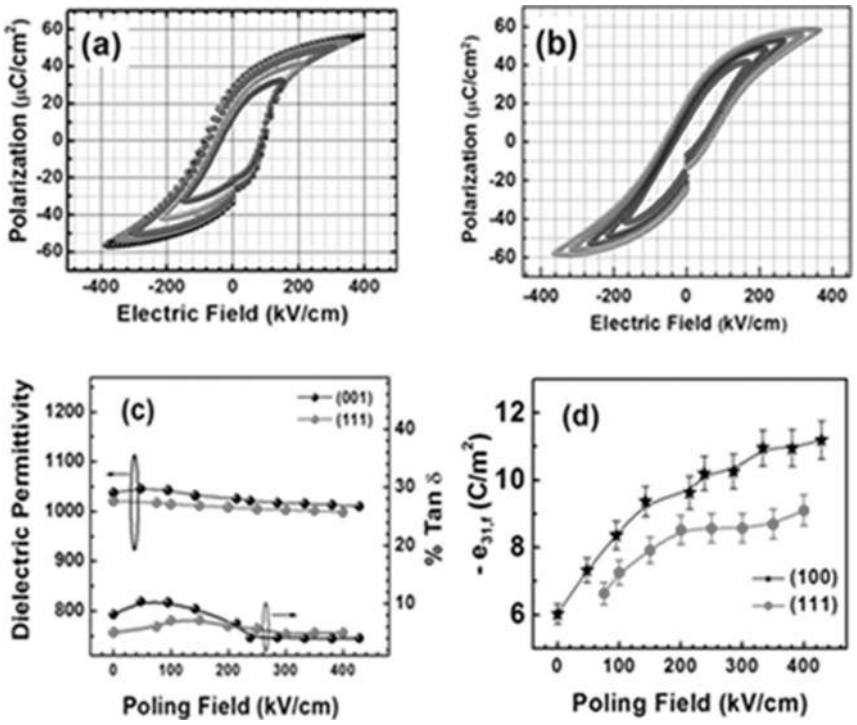

Figure 8. Polarization hysteresis of laser annealed (a) (001) and (b) (111) PZT thin films. (c) Dielectric permittivity and loss tangents and (d) piezoelectric $e_{31,f}$ results as a function of poling field for laser annealed (001) and (111) textured PZT thin films [14].

and (001)$PbTiO_3$/Pt/ Ti/SiO_2/Si substrates. It was shown that by minimizing nucleation energy with suitable buffer layers, PZT films can be grown in preferred orientation at relatively low temperatures (350–375°C) with good functional properties for thin-film MEMS applications (**Figure 8**). Both (001) and (111) oriented PZT films exhibited relatively good ferroelectricity with large P_r (31 and 24 μC/cm² for (001) and (111) PZT, respectively) and small E_c (86 and 64 kV/cm for (001) and (111) PZT, respectively). The maximum $e_{31,f}$ piezoelectric charge coefficients are ~11 and 9 C/m² for (001) and (111) PZT thin films, respectively. However, in this case, particular sputtered amorphous PZT films were needed.

Considering productivity, a semiconductor diode laser is preferred because of its low cost, small size, and low energy consumption, compared with conventional solid state, CO_2 or excimer lasers. Chen et al. recently reported a method that can be used to crystallize PZT films derived from sol-gel solution on either Pt or Li-Nb-O-coated Si substrate by LA treatment using a 980 nm continuous wave semiconductor laser [35, 36]. From dielectric constant measurement, it is found that one LA process generates 45-nm-thick crystallized PZT layer. The dielectric constant of the PZT film is about 1200, which is comparable to that of PZT films prepared by conventional RTA technique. However, the substrate temperature required for LA-crystallized PZT film by this method is relatively high (~500°C).

2.2.3. Microwave-assisted annealing (MV)

Microwave is an electromagnetic wave with wavelength ranging between 1 and 1 mm and frequency ranging from 1 to 300 GHz [37]. The difference between conventional furnace thermal annealing and MV annealing is the mechanism of these two methods. The thermal approach sinters samples by transferring heat through objects via thermal conduction. Thus, the heating source of this technique is the furnace. However, the MV annealing is different. The materials absorb the electromagnetic energy and transform it into heat to increase the temperature. Therefore, the heating source is materials themselves.

Recently, the MV processing has been gaining great attention for various types of materials including ceramics and metal-oxide thin films. Compared to the conventional thermal annealing technique, the MV heating offers more thermal uniformity, lower annealing temperature, shorter processing time with extremely high rate, and reduced grain growth [38]. MW-annealing techniques were applied for crystallization of PZT films at relatively low temperatures (<500°C) [13, 39–42]. For instance, Wang et al. reported a crystallization study of sol-gel $Pb(Zr_{0.45}Ti_{0.55})O_3$ films on platinized Si substrates, pyrolyzed at 400°C, and heated at 430–450°C for 30 min, using a single-mode 2.45 GHz microwave irradiation system in a magnetic field. Good ferroelectric response was obtained upon heating the films at/above 450°C [13] (**Figure 9**). It was found that the MV-annealed PZT films first crystallized into an intermediate pseudo-perovskite phase at 430°C, and then mostly crystallized into the perovskite phase at 450°C. This phenomenon was not observed in PZT films prepared by conventional thermal processing. The crystallization of amorphous PZT films by MV annealing is due to the heat originated from the substrate together with direct MV irradiation onto the films.

Although, the densification of the MV-annealed films is much higher than the conventional thermal process with the same temperature and duration, some fundamental issues limit wide usage of the MV-annealed PZT films. That is because the PZT can only absorb waves with a specific range of frequency, which limits the tools to high frequency (>25 GHz). However, most commercialized MV tools are at approximately 2.4 GHz, which lead to low MV absorption of PZT. Therefore, either preheating is used or absorption aids are added to increase the efficiency of sintering. For example, Sharma et al. added carbon powder in the PZT film to enhance the absorption [43]. Additionally, because the heat is generated internally, the

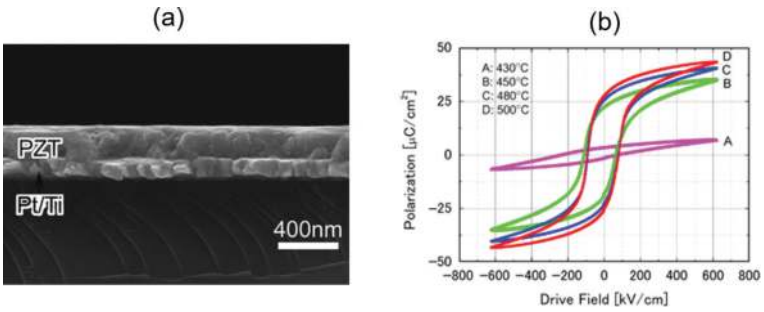

Figure 9. (a) SEM image of PZT film crystallized by MV at 450°C. (b) Hysteresis loops of PZT films crystallized by MV at different temperatures [13].

http://dx.doi.org/10.5772/intechopen.79378

volume of material is determining the heat generation. For a nonuniform film, the heat would generate nonuniformly and result in nonuniform property, and even cracks in the films.

2.2.4. Flash-lamp annealing

The photonic sintering is a technique that uses a broadband (UV to IR), short (<ms) and high-intensity pulse generated from a xenon gas-filled flash-lamp to heat the films. The thermal budget transferred to the film and substrate can be controlled by the pulse duration allowing PZT sintering while minimizing substrate heating. This unique annealing technique enables a direct formation of perovskite PZT film on low melting point substrates. Amorphous PZT films were successfully transformed to perovskite phase by a flash lamp annealing technique (energy of 27 J/cm^2) with a crystallization time of 1.2 ms at a substrate temperature of 350°C [44]. Granular

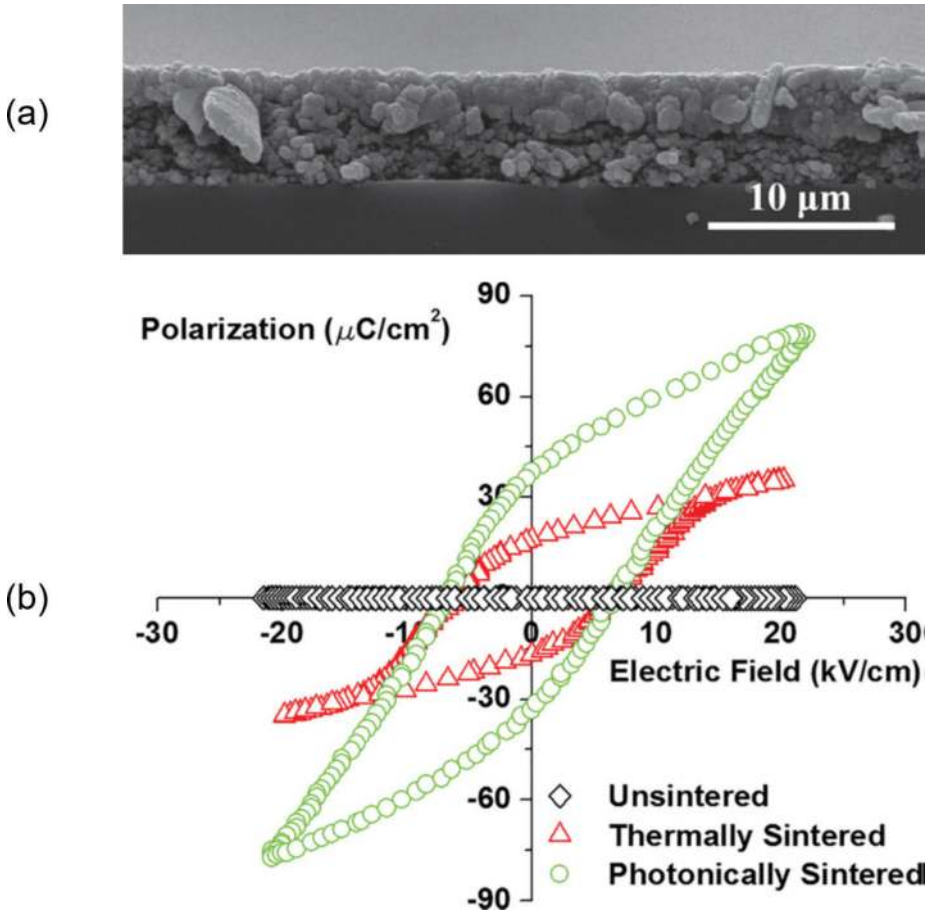

Figure 10. (a) Cross-sectional SEM image of photonically sintered PZT film on stainless steel substrate. (b) Low-frequency hysteresis loop shows that photonically sintered (green) PZT film has superior remanent polarization (32.4 μC/cm^2) than the thermally sintered (red) film (17.1 μC/cm^2) [45].

PZT grains were observed on various kinds of electrodes (Pt, Ru, RuO_2), which indicates that crystal growth begins from the film surfaces. However, the small local sintering area (μm to mm scale) precludes applications with large feature sizes.

Recently, Borkholder et al. demonstrated a new method of printing and sintering microscale PZT films with low substrate temperature increase [45]. PZT ink was aerosol-jet printed on either stainless steel or PET substrates. After drying at 200°C for 2 h in vacuum, the printed PZT gel was photonically sintered using repetitive sub-ms pulses of high-intensity broad spectrum light in an atmospheric environment. The highest measured substrate temperature was 170°C. The obtained P_r and E_c were 32.4 μC/cm^2 and 6.7 kV/cm, respectively (**Figure 10**).

3. Micro/nanoscale patterning of PZT films

3.1. Etching process

3.1.1. Physical dry etching

Dry-etching process with a high etch rate, high selectivity to electrode material, and vertical etch profile is preferable for patterning PZT films. Recently, many researchers have studied the etching of PZT films using halogen gases with various etching systems such as reactive ion etching (RIE) [46, 47] and inductively coupled plasma (ICP) [48, 49]. The main problem in the dry etching of PZT films is that the vapor pressures of the etch by-product (mainly metal halogen compounds) are low. Furthermore, the metal halogen compounds have different vapor pressures, which cause compositional variation in the multicomponent PZT films [50]. The etching of PZT films has been studied more widely in chlorinated plasma than in fluorinated plasma because of high vapor pressure of metal chlorides compared with fluoride counterparts. Lee et al. [49] studied the dry-etching mechanism of PZT films in high-density CF_4 and Cl_2/CF_4 ICP. The etching of PZT films in CF_4-based plasma is chemically assisted sputter etching, and the dominant step of the overall etching process is either the formation or the removal of the etch by-products, depending on the etching conditions. The etching of PZT films in Cl_2/CF_4 mixed plasma is mainly dominated by the formation of metal chlorides, which depends on the concentration of the atomic Cl and the bombarding ion energy. The PZT film showed a maximum etch rate in 90% $Cl_2/(Cl_2/CF_4)$ plasma where the concentration of atomic Cl was maximum (**Figure 11(a)**). The amount of sidewall residue was greatly reduced in Cl_2/CF_4 mixed plasma compared with in CF_4 plasma. A more vertical etch profile of PZT films was obtained by lowering the process pressure and increasing the substrate bias voltage (**Figure 11(b)**). However, the plasma etch process degrades the structural and electrical properties because of physical damage and chemical residue contamination. The physical damage caused by the bombardment of energetic charged ions to the film surface, which alters the near-surface region and changes its electrical properties. The surface contamination by the etch by-products and penetration of mobile ions into the bulk may also degrade film's quality. Later, Kim et al. reported both a reduction in the etching damage to PZT films during etching in a Cl_2/CF_4 plasma with Ar or O_2 added and the recovery of etching damage by using O_2 annealing [51].

http://dx.doi.org/10.5772/intechopen.79378

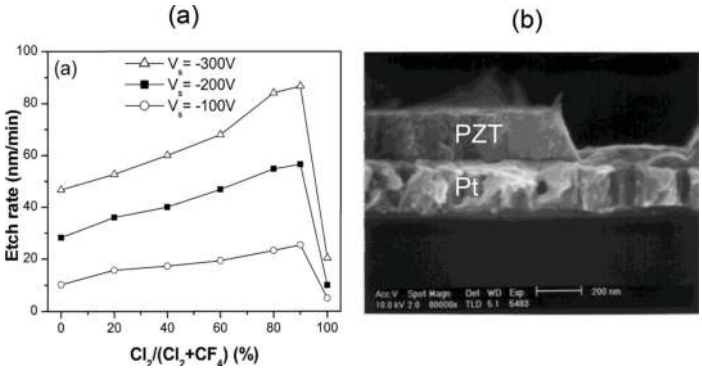

Figure 11. (a) The etching rate of PZT films as a function of $Cl_2/(Cl_2 + CF_4)$ concentration. (b) Cross-sectional SEM image of PZT pattern [49].

3.1.2. Chemical wet etching

Wet etching is an effectively alternative technique for PZT film's patterning due to its high etching rate, low cost, and high selectivity. Since, PZT can be regarded as a compound of PbO, ZrO_2 and TiO_2, etchants containing several compositions are demanded for PZT thin film etching. In recent years, many studies have been performed on wet etching of PZT films using mixtures of various acids, following single-or two-step processes [39, 52–56]. However, problems such as fast etch rate (>400 nm/min), severe undercut, and formation of higher etch residue were encountered. Wang et al. introduced a two-step wet-etching process, using buffered HF acid (BHF) in the first step, and 2HCl:H_2O at 45°C in the second step, to etch PZT films [54]. However, significant undercutting and brim damage were observed in the achieved pattern. Later, a novel wet-etching process was proposed using 1BHF:2HCl:4NH_4Cl:4H_2O solution as the etchant, where NH_4 was used as an additive to decrease the undercutting of the obtained PZT pattern. Using this technique, PZT patterns with acceptable undercutting (1.5:1) can be obtained.

Ezhilvalavan et al. proposed a wet-etch recipe using 25% [BOE:HCl:CH_3COOH:HNO_3:NH_4Cl:EDTA ethylenediamine tetra acetate trihydrate]:75% H_2O to pattern PZT films [39]. The etch recipe provided a high etch rate (200 nm/min) and high selectivity with respect to photoresist, limited undercutting (1.5:1, lateral:thickness), and effectively removed the residues on the etched surfaces. Using this recipe, a high-quality patterned PZT film was obtained with a large P_r of 30 μC/cm^2, a E_c of 150 kV/cm (**Figure 12**), fatigue-free characteristics, and a low leakage current density of 10^{-6} A/cm^2 at 200 × 10^5 kV/cm. Although various wet-etching procedures have been attempted, the details of the etching mechanism and residue stripping are not properly explained, and more importantly, the ferroelectric/piezoelectric characteristics of the etched PZT structures and its electrical reliability tests have not been studied in details.

3.2. Lift-off process

Compared to the etching technique, lift-off process is preferable since it has not suffered from the physical and chemical damages caused by etch plasma. The pattern ability of PZT films

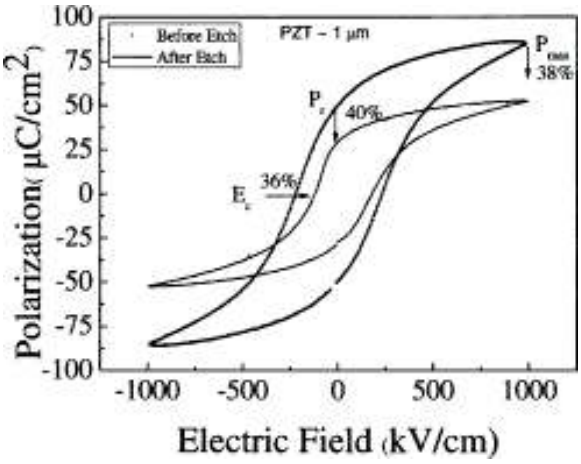

Figure 12. Hysteresis loop of the 1-μm-thick PZT film patterned by a wet-etch process [39].

by lift-off process using thick photoresist [57], hydrophobic self-assembly-monolayer, or thin ZnO film [58] as a sacrificial layer was already proved. However, the feature size was mostly limited above 50 μm, and also PZT films exhibited random crystalline structure, large leakage current, and rather poor ferroelectric properties. Recently, Tue et al. demonstrated sub-5 μm pattern of sol-gel-derived PZT films with a thickness of 80–390 nm by a novel lift-off process using solution-processed amorphous metal oxides as a sacrificial layer (**Figure 13**) [59]. The process includes three steps as follows: (1) deposition and patterning of the sacrificial lift-off layer (In-Zn-O), (2) PZT spin coating, and (3) etching of the sacrificial layer for PZT lift-off. It was found that the amorphous In-Zn-O layer acted as a good barrier between the Pt substrate and PZT film, inhibiting the crystallization of PZT film. In addition, the In-Zn-O film can be easily removed by a wet etching leading to a clean and smooth surface. As a result, the lift-off PZT film exhibited better ferroelectric properties, higher breakdown endurance, and more well-defined shape compared with the wet-etched ones.

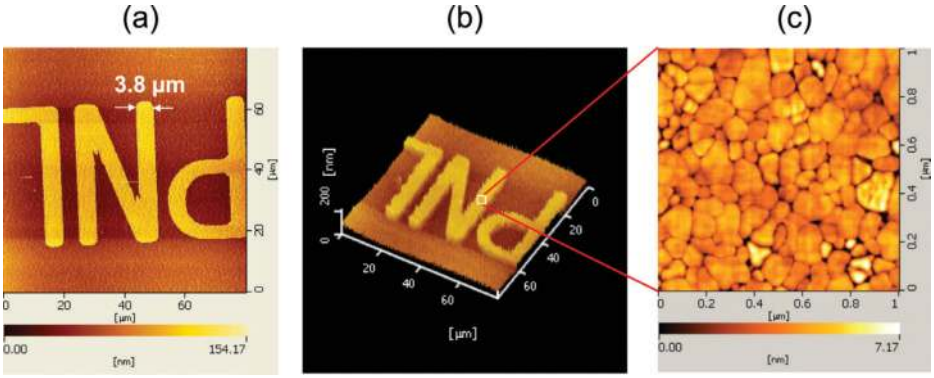

Figure 13. AFM image of fine PZT pattern: (a) 2D morphology, (b) 3D morphology, and (c) local surface morphology [59].

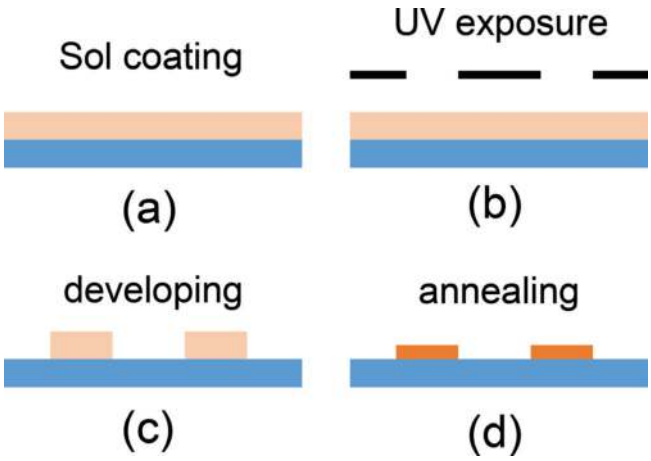

Figure 14. Scheme for patterning of PZT thin film by ultraviolet (UV) light.

3.3. Direct UV-patterning

A general scheme for patterning of PZT thin film by a UV light is shown in **Figure 14**, which is similar to a photoresist patterning process. An UV-sensitive PZT sol is first synthesized, and then spin-coated on a substrate without thermal drying step. After that, the gel film is irradiated under the UV light through a mask for photolysis step. The pattern on the mask will be transferred to PZT film according to the exposed and unexposed area. After the photolysis, the PZT film is placed in a nonionic surfactant solution to remove the unexposed area and is sintered for crystallization.

Many studies have reported the use of UV light for direct patterning PZT thin films using photosensitive PZT sol solutions [60–64]. Calzada et al. synthesized photo-sensitive $PbTiO_3$ solutions, which have a maximum of absorption in UV between 200 and 300 nm [60]. Weihua et al obtained an UV photosensitive PZT sol using chemical modification in acetylacetone [61]. Marson et al. developed a highly concentrated solution for producing photo-patternable layers of PZT by dissolving an amorphous PZT powder into acrylic acid [62]. Although ferroelectric/piezoelectric properties of PZT films patterned by the UV-light are comparable to those of conventional PZT thin films, they normally require complicated modification of the precursor solution, and also feature sizes of PZT patterns are relatively large (in the order of tens of micrometers).

3.4. Direct nanoimprinting lithography (NIL)

Since the first development in 1995, the nanoimprint lithography (NIL) has become one of the advanced patterning methods for nanofabrication. The idea of NIL is to transfer patterns by pressing a designed master mold into resist [65]. NIL overwhelms other lithographic processes by its low cost, high throughput, and high resolution. Various kinds of functional materials can be textured by NIL, and functional devices are obtained accordingly.

Li et al. reported pattern transfer of nanoscale ferroelectric PZT gratings on a platinized substrate by a reversal NIL without any chemical etch processes [66]. PZT sol was spin coated onto

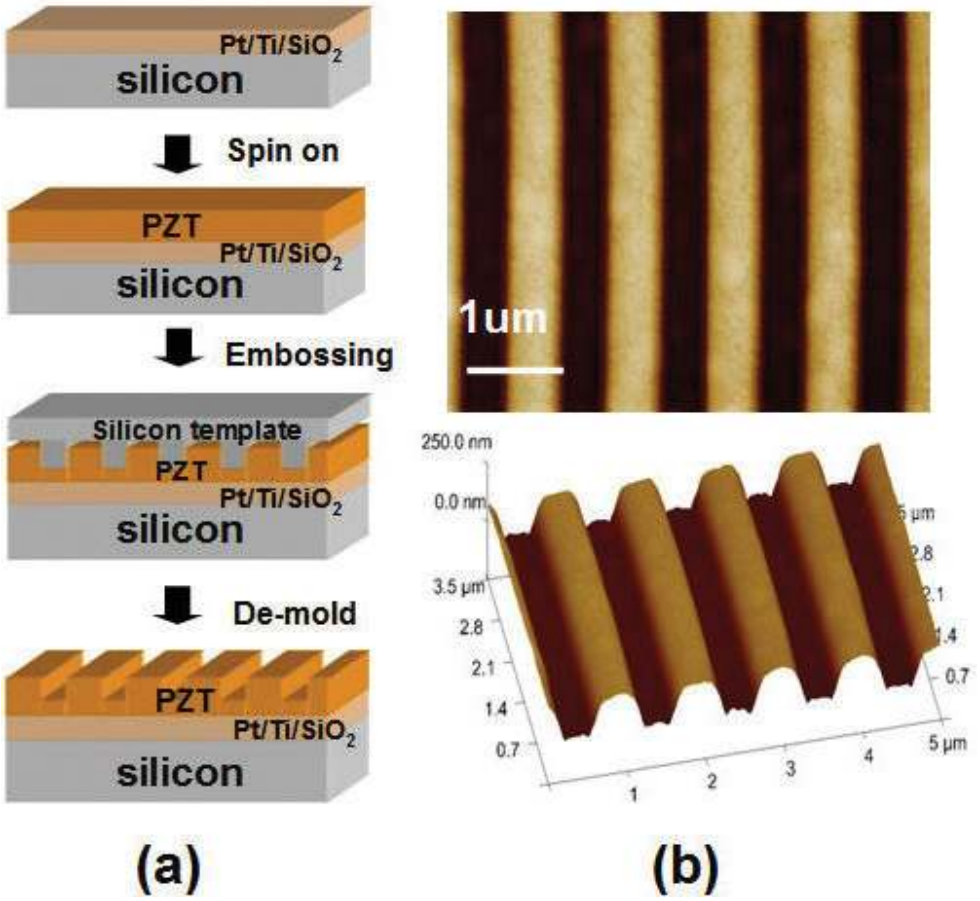

Figure 15. PZT films nanoembossing process and results of embossed profiles. (a) A schematic diagram illustrating a one-step embossing process to form a stagger shape in a PZT film with two different thicknesses and (b) AFM images of embossed stagger like profiles of PZT film [67].

a template with an antistick layer. The template with PZT was then placed onto the substrate and applied a pressure. After that, the substrate was separated from template directly. The transferred sample was then crystallized by thermal annealing in air at 650°C for 15 min. The patterned lines appeared to be reasonably straight and well ordered with few defects. The height of the gratings was in the range between 125 and 250 nm depending on the template mold.

Shen et al applied a nanoembossing technique to form a stagger structure in PZT film [67]. **Figure 15(a)** illustrates the nanoembossing process of PZT film. **Figure 15(b)** displays the embossed PZT film profiles measured by AFM; showing an embossed depth of about 160 on a 450-nm thick PZT film with well-quadrate-patterned profiles. After crystallization, the PZT films exhibited a tetragonal structure with (111) preferred orientation. In addition, the morphology of the embossed region remained stable. Chen group demonstrated a low-press, low-temperature direct NIL method for patterning PZT films [68, 69]. In general, conventional direct NIL utilizes ultrahigh pressure or temperature to form patterns on the film. The

use of a sharp-tip mold combined with an underlying soft gel film may overcome issues of the conventional NIL. This approach is more favorable because of its simplicity and reduced temperature as well as imprinting pressure. Besides, imprinting on the gel film instead of on the bulk film makes the NIL much easily to be carried out. It was also successfully demonstrated that the NIL on the metal/ferroelectric bilayer structure would help to overcome the flattened problem of pattern in a gel film. Moreover, the metal film prevents the mold from directly contacting with the PZT gel. Therefore, no residual or contaminant will be observed on the mold.

4. Applications of low-temperature-processed PZT films

Thanks to multifunctional properties, PZT films can be utilized for various applications in sensor, actuator, nonvolatile memory, and energy harvesting as well. Once PZT films can be deposited at a low temperature, which is compatible with Si technology, direct integration of PZT films to other active control element, i.e., Si-CMOS, becomes possible. Further lowering of PZT process temperature to be compatible with flexible substrates enables flexible PZT-based electronics. This part briefly summarizes emerging applications of low-temperature PZT films.

4.1. Piezoelectric actuator

A diaphragm-type piezo actuator was demonstrated using a low-temperature (450°C) solution-processed PZT film [15]. Cross-sectional structure and SEM image of the fabricated actuator is given in **Figure 16(a)** and **(b)**. The observed experimental data agreed well with simulation result in which the actuator displacement linearly increased as the increase of applied voltage (**Figure 16(c)**). The maximum displacement was approximately 130 nm at 10 V. These results verify that the low-temperature-processed PZT film can be applied for actuator applications.

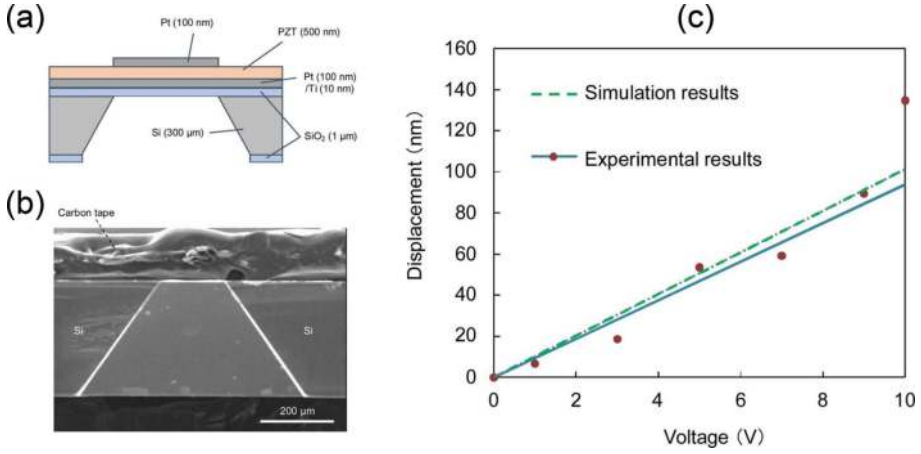

Figure 16. (a) Cross-sectional structure and (b) SEM image of the fabricated PZT actuator. (c) Comparison of the displacement between experiment and simulation results [15].

4.2. Piezoelectric energy harvester

Energy harvesting, which collects useful energy from wasted energy sources, is the most promising technology to provide solutions for the shortage of a fossil fuel, various environmental problems, and the improvement of energy efficiency in smart grids. Piezoelectric energy harvesters have been actively studied due to their easy integration with MEMS and integrated circuit technologies [70–74]. The cantilever type is the most typical structure of a piezoelectric energy harvester, in which a piezoelectric material is deposited onto a rigid Si cantilever, and a proof mass is located at the free end of the cantilever. The electricity can be generated by a conversion of kinetic energy from the mechanically stimulated proof mass via the piezoelectric material. However, the typical rigid-body-based cantilever type energy harvester has a large resonance frequency due to its high spring constant. Thus, it is not for harvesting energy from human activity or low-frequency ambient vibration. In this regard, flexible PZT appears as a promising candidate for flexible energy harvesting applications.

Cho et al. presented a microfabricated flexible and curled PZT cantilever using d_{33} piezoelectric mode for vibration-based energy harvesting applications [70]. The proposed energy harvester consists of PI layer, PZT thin film, and interdigitated IrO_x electrodes. The PZT thin film on PI layer showed $2P_r$ and $2E_c$ of approximately 47.9 μC/cm^2 and 78.8 kV/cm, respectively. At optimal conditions of resistive load (6.6 MΩ) and resonant frequency (97.8 Hz), the fabricated

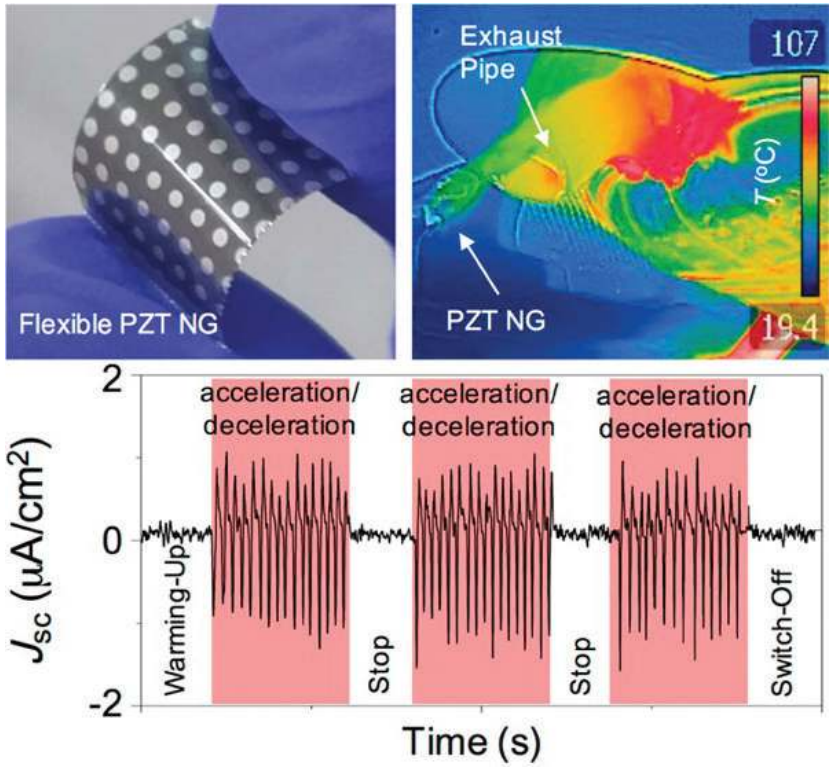

Figure 17. Illustration of flexible PZT film-based NG [74].

device was able to generate output voltage and power of 1.2 V and 117 nW, respectively. Through the introduction of indium-tin-oxide (ITO) and polyethylene terephthalate (PET) substrates to laser lift-off PZT-based energy harvester, a transparent flexible device (TFD) was implemented [71]. The TFDs based on PZT films generated an AC-type output signal and output power of 8.4 nW/cm^2, at periodically bending and releasing motion.

Recently, single-cell hybrid nanogenerators (NGs) that can simultaneously harvest mechanical and thermal energies have received great attention [72–74]. Jung group reported the development of a hybrid piezoelectric-pyroelectric NG using PZT material to simultaneously harvest mechanical and thermal energies from extreme resources [74]. By the combination of perovskite $LaNiO_3$ and Ni-Cr metal foil as a bottom electrode and a flexible substrate, they have successfully grown a PZT film with a large P_r (28 μC/cm^2), high piezoelectric constant (140 pC/N), and high pyroelectric coefficient (50 nC/cm^{2}K). The PZT-based NG was proven to stably generate electric power in harsh environment, and at elevated temperatures (**Figure 17**).

The success of flexible piezoelectric energy harvesters lies in its packaging density, output voltage and power, resonance bandwidth, lifetime, and cost. Among these, the two biggest challenges are wider bandwidth and higher power density. Advances in novel piezoelectric materials such as giant coefficient and lead-free piezoelectric as well as harvester structural design are expected to bring us closer to battery-free autonomous systems.

5. Conclusion

This review on low-temperature processing of solution-derived PZT films summarized major approaches to decrease the crystallization temperature below 450°C. The success would mitigate the integration of PZT films in electronics devices and diminish a possible loss of stoichiometry and consequent worsened functional properties due to either evaporation of volatile species (lead-, alkali-oxides) or possible interface reactions. The approaches described here include chemical and physical treatments for the precursor solutions, as-deposited, and as-pyrolyzed films by solvothermal synthesis, UV-light treatment, laser, microwave, and flash-lamp-assisted annealing. It reveals that design of functional precursor solutions, which are photo-sensitive and possibly decomposable at a low temperature, is critical to the production of high-quality PZT films.

Combination of low-temperature solution-processed PZT films with facile micro-/nano-patterning techniques would open new opportunities for low-cost, large-area transparent, flexible ferroelectric/piezoelectric devices such as nonvolatile memory, piezoelectric sensor/actuator/transducer, and energy harvesters.

Acknowledgements

The authors would like to thank JST, ERATO Shimoda Nano-Liquid Process project and JST-CREST project for financial support. Members of the Center for Single Nanoscale Innovative Devices, Japan Advanced Institute of Science and Technology are acknowledged for their technical assistance.

Conflict of interest

The authors declare that they have no competing interests.

Author details

Phan Trong Tue* and Yuzuru Takamura

*Address all correspondence to: phan-tt@jaist.ac.jp

School of Materials Science, Japan Advanced Institute of Science and Technology, Nomi-shi, Ishikawa, Japan

References

[1] Muralt P, Polcawich RG, Trolier-McKinstry S. Piezoelectric thin films for sensors, actuators, and energy harvesting. MRS Bulletin. 2009;**34**(9):658-664

[2] Setter N et al. Ferroelectric thin films: Review of materials, properties, and applications. Journal of Applied Physics. 2006;**100**(5):051606

[3] de Araujo CAP et al. Fatigue-free ferroelectric capacitors with platinum electrodes. Nature. 1995;**374**:627

[4] Park BH et al. Lanthanum-substituted bismuth titanate for use in non-volatile memories. Nature. 1999;**401**:682

[5] Aratani M et al. Epitaxial-grade polycrystalline Pb(Zr,Ti)O_3 film deposited at low temperature by pulsed-metalorganic chemical vapor deposition. Applied Physics Letters. 2001;**79**(7):1000-1002

[6] Schatz A, Pantel D, Hanemann T. Pulsed laser deposition of piezoelectric lead zirconate titanate thin films maintaining a post-CMOS compatible thermal budget. Journal of Applied Physics. 2017;**122**(11):114502

[7] Tsuchiya K, Kitagawa T, Nakamachi E. Development of RF magnetron sputtering method to fabricate PZT thin film actuator. Precision Engineering. 2003;**27**(3):258-264

[8] Maki K et al. Lowering of crystallization temperature of sol-gel derived Pb(Zr, Ti)O_3 thin films. Integrated Ferroelectrics. 2000;**30**(1-4):193-202

[9] Perez J, Vilarinho PM, Kholkin AL. High-quality $PbZr_{0.52}Ti_{0.48}O_3$ films prepared by modified sol–gel route at low temperature. Thin Solid Films. 2004;**449**(1):20-24

[10] Wu A et al. Early stages of crystallization of sol−gel-derived lead zirconate titanate thin films. Chemistry of Materials. 2003;**15**(5):1147-1155

[11] Morita T et al. Ferroelectric properties of an epitaxial lead zirconate titanate thin film deposited by a hydrothermal method below the Curie temperature. Applied Physics Letters. 2004;**84**(25):5094-5096

[12] Il DK, Ho GK. Characterization of highly preferred Pb(Zr,Ti)O_3 thin films on $La_{0.5}Sr_{0.5}CoO_3$ and $LaNi_{0.6}$ $Co_{0.4}O_3$ electrodes prepared at low temperature. Japanese Journal of Applied Physics. 2001;**40**(4R):2357

[13] Wang Z et al. Crystallization of ferroelectric lead zirconate titanate thin films by microwave annealing at low temperatures. Journal of the American Ceramic Society. 2011; **94**(2):404-409

[14] Bharadwaja SSN et al. Highly textured laser annealed Pb($Zr_{0.52}Ti_{0.48}$)O_3 thin films. Applied Physics Letters. 2011;**99**(4):042903

[15] Shimura R et al. Solution-based process with thermal UV treatment for fabrication of piezoelectric PZT films for an actuator array at temperatures under 450°C. Sensors and Actuators A: Physical. 2017;**267**:287-292

[16] Wu A et al. Effect of lead zirconate titanate seeds on Pt_xPb formation during the pyrolysis of lead zirconate titanate thin films. Journal of the American Ceramic Society. 2002; **85**(3):641-646

[17] Wu A et al. Characterization of seeded sol–gel lead zirconate titanate thin films. Journal of the European Ceramic Society. 1999;**19**(6):1403-1407

[18] Chen S-Y, Chen IW. Temperature–time texture transition of Pb($Zr_{1-x}Ti_x$)O_3 thin films: I, role of Pb-rich intermediate phases. Journal of the American Ceramic Society. 1994;**77**(9):2332-2336

[19] Huang Z, Zhang Q, Whatmore RW. The role of an intermetallic phase on the crystallization of lead zirconate titanate in sol–gel process. Journal of Materials Science Letters. 1998;**17**(14):1157-1159

[20] Huang Z, Zhang Q, Whatmore RW. Low temperature crystallization of lead zirconate titanate thin films by a sol-gel method. Journal of Applied Physics. 1999;**85**(10):7355-7361

[21] Guozhang Cao and Ying Wang. Nanostructures and nanomaterials: Synthesis, properties and applications. World Scientific. 2011. ISBN 978-981-4322-50-8

[22] Yoshimura M, Byrappa K. Hydrothermal processing of materials: Past, present and future. Journal of Materials Science. 2008;**43**(7):2085-2103

[23] Katsuhiko S et al. Preparation of lead zirconate titanate thin film by hydrothermal method. Japanese Journal of Applied Physics. 1991;**30**(9S):2174

[24] Takayuki K et al. Bending actuator using lead zirconate titanate thin film fabricated by hydrothermal method. Japanese Journal of Applied Physics. 1992;**31**(9S):3090

[25] Morita T, Kanda T, Yamagata Y, Kurosawa M, Higuchi T. Single process to deposit lead zirconate titanate (PZT) thin film by a hydrothermal method. Japanese Journal of Applied Physics. 1997;**36**:2998-2999

[26] Chien AT, Speck JS, Lange FF. Hydrothermal synthesis of heteroepitaxial $Pb(Zr_xTi_{1-x})O_3$ thin films at 90-150°C. Journal of Materials Research. 1997;**12**(5):1176-1178

[27] Oledzka M et al. Influence of precursor on microstructure and phase composition of epitaxial hydrothermal $PbZr_{0.7}Ti_{0.3}O_3$ films. Chemistry of Materials. 2003;**15**(5):1090-1098

[28] Morita T et al. Ferroelectric property of an epitaxial lead zirconate titanate thin film deposited by a hydrothermal method. Journal of Materials Research. 2004;**19**(6):1862-1868

[29] Li J et al. A low-temperature crystallization path for device-quality ferroelectric films. Applied Physics Letters. 2010;**97**(10):102905

[30] Kim YH et al. Flexible metal-oxide devices made by room-temperature photochemical activation of sol–gel films. Nature. 2012;**489**:128-132

[31] Umeda K et al. Impact of UV/O_3 treatment on solution-processed amorphous $InGaZnO_4$ thin-film transistors. Journal of Applied Physics. 2013;**113**(18):184509

[32] Yue J et al. UV-assisted low-temperature sol–gel deposition of $Pb(Zr_{0.4}Ti_{0.6})O_3$ film and its photoelectrical properties. Journal of Sol-Gel Science and Technology. 2017;**83**(3):647-652

[33] Bretos I et al. Activated solutions enabling low-temperature processing of functional ferroelectric oxides for flexible electronics. Advanced Materials. 2014;**26**(9):1405-1409

[34] Bretos I et al. Active layers of high-performance lead zirconate titanate at temperatures compatible with silicon nano- and microelectronic devices. Scientific Reports. 2016;**6**: 20143

[35] Yagi XCAM. Development of crystallization of PZT films by laser annealing. Ricoh Technical Report. 2014;**39**:06

[36] Miyazaki T et al. Low-temperature crystallization of CSD-derived PZT thin film with laser annealing. Materials Science and Engineering B. 2010;**173**(1):89-93

[37] Katz JD. Microwave sintering of ceramics. Annual Review of Materials Science. 1992; **22**(1):153-170

[38] Agrawal DK. Microwave processing of ceramics. Current Opinion in Solid State and Materials Science. 1998;**3**(5):480-485

[39] Wang ZJ et al. Low-temperature growth of high-quality lead zirconate titanate thin films by 28 GHz microwave irradiation. Applied Physics Letters. 2005;**86**(21):212903

[40] Bhaskar A et al. Low-temperature crystallization of sol–gel-derived lead zirconate titanate thin films using 2.45 GHz microwaves. Thin Solid Films. 2007;**515**(5):2891-2896

[41] Ankam B et al. Effect of microwave annealing temperatures on lead zirconate titanate thin films. Nanotechnology. 2007;**18**(39):395704

[42] Wang ZJ et al. Low-temperature growth of ferroelectric lead zirconate titanate thin films using the magnetic field of low power 2.45 GHz microwave irradiation. Applied Physics Letters. 2008;**92**(22):222905

[43] Pramod KS et al. Dielectric and piezoelectric properties of microwave sintered PZT. Smart Materials and Structures. 2001;**10**(5):878

[44] Koji Y et al. Novel Pb(Ti, Zr)O_3 (PZT) crystallization technique using flash lamp for ferroelectric RAM (FeRAM) embedded LSIs and one transistor type FeRAM devices. Japanese Journal of Applied Physics. 2002;**41**(4S):2630

[45] Ouyang J et al. Photonic sintering of aerosol jet printed lead zirconate titanate (PZT) thick films. Journal of the American Ceramic Society. 2016;**99**(8):2569-2577

[46] Bale M, Palmer RE. Reactive ion etching of piezoelectric Pb(Zr_xTi_{1-x})O_3 in a SF_6 plasma. Journal of Vacuum Science & Technology, A: Vacuum, Surfaces, and Films. 1999;**17**(5):2467-2469

[47] Wang S et al. Deep reactive ion etching of lead zirconate titanate using sulfur hexafluoride gas. Journal of the American Ceramic Society. 1999;**82**(5):1339-1641

[48] Chee Won C, Chang Jung K. Etching effects on ferroelectric capacitors with multilayered electrodes. Japanese Journal of Applied Physics. 1997;**36**(5R):2747

[49] Jin-Ki J, Won-Jong L. Dry etching characteristics of Pb(Zr,Ti)O_3 films in CF_4 and Cl_2/CF_4 inductively coupled plasmas. Japanese Journal of Applied Physics. 2001;**40**(3R):1408

[50] Masaru O et al. Metalorganic chemical vapor deposition of c-axis oriented PZT thin films. Japanese Journal of Applied Physics. 1990;**29**(4R):718

[51] Kang M-G, Kim K-T, Kim D-P, Kim C-I. Reduction of dry etching damage to PZT films etched with a Cl-based plasma and the recovery behavior. Journal of the Korean Physical Society. 2002;**41**(4):6

[52] Mancha S. Chemical etching of thin film PLZT. Ferroelectrics. 1992;**135**(1):131-137

[53] Miller RA, Berwnstein JJ. A novel wet etch for patterning lead zirconate-titanate (PZT) thin-films. Integrated Ferroelectrics. 2000;**29**(3-4):225-231

[54] Wang LP et al. Wet-etch patterning of lead zirconate titanate (PZT) thick films for microelectromechanical systems (MEMS) applications. MRS Proceedings. 2000;**657**:EE5.39

[55] Kelu Z, Jian L, Jiaru C. A novel wet etching process of Pb(Zr,Ti)O_3 thin films for applications in microelectromechanical system. Japanese Journal of Applied Physics. 2004;**43**(6S):3934

[56] Che L, Halvorsen E, Chen X. An optimized one-step wet etching process of Pb($Zr_{0.52}Ti_{0.48}$)O_3 thin films for microelectromechanical system applications. Journal of Micromechanics and Microengineering. 2011;**21**(10):105008

[57] Zhao HJ, Ren TL, Liu JS, Liu LT, Li ZJ. Fabrication of high quality PZT thick film using lift-off technique. In: Technical Proceedings of the 2003 Nanotechnology Conference and Trade Show, Vol. 1; 2003. p. 4

[58] Li J et al. Micro-patterning of PZT thick film by lift-off using ZnO as a sacrificial layer. Ceramics International. 2015;**41**(6):7325-7328

[59] Tue PT, Shimoda T, Takamura Y. Fine-patterning of sol-gel derived PZT film by a novel lift-off process using solution-processed metal oxide as a sacrificial layer. Ceramics International. 2016;**42**(16):18431-18435

[60] Calzada ML et al. Photo-sensitive sol-gel solutions for the low-temperature UV-assisted processing of $PbTiO_3$ based ferroelectric thin films. Journal of Materials Chemistry. 2003;**13**(6):1451-1457

[61] Weihua Z, Gaoyang Z, Zhiming C. Photosensitive PZT gel films and their preparation for fine patterning. Materials Science and Engineering B. 2003;**99**(1):168-172

[62] Marson S et al. Direct patterning of photosensitive chemical solution deposition PZT layers. Journal of the European Ceramic Society. 2004;**24**(6):1925-1928

[63] Kang GY et al. Fabrication and electromechanical properties of a self-actuating $Pb(Zr_{0.52}Ti_{0.48})O_3$ microcantilever using a direct patternable sol-gel method. Applied Physics Letters. 2006;**88**(4):042904

[64] Kumar SR et al. Control of microstructure and functional properties of PZT thin films via UV assisted pyrolysis. Journal of Sol-Gel Science and Technology. 2007;**42**(3):309-314

[65] Chou SY, Krauss PR, Renstrom PJ. Imprint of sub-25 nm vias and trenches in polymers. Applied Physics Letters. 1995;**67**(21):3114-3116

[66] Li Z-D et al. Pattern transfer of nano-scale ferroelectric PZT gratings by a reversal nano-imprint lithography. Microelectronic Engineering. 2011;**88**(8):2037-2040

[67] Shen Z et al. Nano-embossing technology on ferroelectric thin film $Pb(Zr_{0.3},Ti_{0.7})O_3$ for multi-bit storage application. Nanoscale Research Letters. 2011;**6**(1):474

[68] Hsieh KC et al. Directly patterning ferroelectric films by nanoimprint lithography with low temperature and low pressure. Journal of Vacuum Science & Technology, B: Microelectronics and Nanometer Structures--Processing, Measurement, and Phenomena. 2006;**24**(6):3234-3238

[69] Chen HL et al. Using direct nanoimprinting of ferroelectric films to prepare devices exhibiting bi-directionally tunable surface plasmon resonances. Nanotechnology. 2008; **19**(43):435304

[70] Cho H, Park J, Park JY. Micro-fabricated flexible PZT cantilever using d33 mode for energy harvesting. Micro and Nano Systems Letters. 2017;**5**(1):20

[71] Do YH et al. Preparation on transparent flexible piezoelectric energy harvester based on PZT films by laser lift-off process. Sensors and Actuators A: Physical. 2013;**200**:51-55

[72] Lee JH et al. Highly stretchable piezoelectric-pyroelectric hybrid nanogenerator. Advanced Materials. 2014;**26**(5):765-769

[73] Yang Y et al. Flexible hybrid energy cell for simultaneously harvesting thermal, mechanical, and solar energies. ACS Nano. 2013;**7**(1):785-790

[74] Ko YJ et al. Flexible $Pb(Zr_{0.52}Ti_{0.48})O_3$ films for a hybrid piezoelectric-pyroelectric nanogenerator under harsh environments. ACS Applied Materials & Interfaces. 2016;**8**(10): 6504-6511